Science and Engineering Research Council
Rutherford Appleton Laboratory
CHILTON, DIDCOT, OXON, OX11 0QX

RAL-85-032

Thermal Neutron Beamline Monitor

P L Davidson

April 1985

RAL 85 032

THERMAL NEUTRON BEAMLINE MONITOR

P L Davidson

Abstract

A detector has been developed which has characteristics that make it suitable for use as a neutron beamline monitor on the Spallation Neutron Source. Efficiency has been reduced to 10^{-4}, pulse pair resolution is 50 nSecs and it presents minimal obstruction to the neutron beam.

THERMAL NEUTRON BEAMLINE MONITOR

CONTENTS

Figure Captions

1. INTRODUCTION

This report describes a novel design of scintillator-based neutron detector, developed specifically to monitor the beams of thermal and epithermal neutrons produced by the Spallation Neutron Source.

A monitor must provide continuous information about the intensity of the neutron beam as a function of time without significantly interfering with it. To achieve this the ideal detector would have a simple efficiency Vs energy relationship and would present the very minimum obstruction to the neutron beam.

Traditionally, on reactor sources, fission monitors are used. In this type of detector a very thin layer of fissile material, commonly ^{235}U, is deposited on a thin substrate and although giving excellent signal to noise ratio, these detectors are slow, and have a complex efficency Vs energy spectrum at epithermal energies.

Low pressure G-M tubes are one alternative but again are rather slow and the thickness of the detector can lead to problems with time resolution when used in time of flight applications.

The design described here has a smooth relationship of efficiency Vs energy, which approximates to $\frac{1}{\sqrt{E}}$ for energies of a few volts, is fast, and is cheap to produce.

2.1 DESIGN CONSIDERATIONS

There are two main factors that determine the design of the monitor detector. First, as a neutron can be detected once only, it follows that the efficiency must be low, in order not to reduce the beam intensity significantly. Second, as the beam intensity is high, care must be taken to ensure that the detector and electronics can cope with the neutron detection rate and that the data acquisition system is not overloaded.

2.2 SNS BEAMLINE NEUTRON INTENSITIES

At 1 eV $I = \frac{7 \times 10^{12}}{L^2 \text{ cms}}$ n/eV.cm^2.s time averaged

at 10 metres from moderator 1μs ≡ 2.77 x 10^{-3} eV.

Therefore $I = \frac{7 \times 10^{12} \times 2.77 \times 10^{-3}}{1000^2}$

$= 1.94 \times 10^4$ n/μS.cm^2.s.

Therefore at 50 Hz the neutron intensity in the pulse

$= \frac{1.94 \times 10^4}{50}$

$= 3.9 \times 10^2$ n/μS.cm^2

For a monitor of area 5 x 4 cms

Neutron countrate $= 7.8 \times 10^3$ n/μS

$= 7.8 \times 10^9$ n/S during the pulse.

Therefore to count at 1 MHZ

Detector efficiency $= \frac{10^6}{7.8 \times 10^9}$

$= 1.3 \times 10^{-4}$

However, obtaining a reliable and repeatable efficiency this low is not straightforward.

2.3 DESIGN FOR LOW EFFICIENCY

The normal efficiency of standard GS20 neutron scintillator glass, 1 mm thick, is 0.5 at 0.1 eV; this must be reduced by a factor of about 5000. There are several possible ways in which this can be achieved, but the following methods are the most obvious ones to consider.

1. Scintillator containing very small quantities of Li^6.

2. Very thin sheets of standard scintillator.

3. An even distribution of small scintillator cubes to sample the beam area.

Considering the methods above, it is apparent that there are practical difficulties with all of them:

1. In order not to change the general characteristics of the scintillator glass significantly, the proportion of lithium must remain unchanged. Therefore to reduce the proportion of Li^6, a mixture of Li^6 and Li^7 must be used in which the Li^6 component is reduced to .002%.

   Natural lithium contains about 7% Li^6, and purified Li^7 contains a residual of about .05% of Li^6, which renders this approach impossible.

2. The thickness of a sheet of scintillator would have to be reduced to about 2 microns to reach the required efficiency level, this is clearly impractical. Also, as the alpha and triton particles, produced by the neutron interaction with the Li^6, have an approximate range of 8 microns and 40 microns respectively, they would therefore escape from the scintillator before depositing all their available energy; this would result in a poor neutron pulse height spectrum and a correspondingly poor countrate stability.

3. This method offers a practical solution to the problem, in which the detection efficiency is given by

   $$\eta = \left(1 - \exp - (2.375\ x/\sqrt{E})\right)\ n\ a/A$$

   where x = scintillator thickness in cms.
   E = neutron energy in eV.
   n = number of scintillator cubes.
   a = area of scintillator cubes.
   A = area of detector.

   For cubes of .25 mm sides arranged in a matrix of 8 mm x 8 mm, the efficiency for neutrons of energy = 0.1 eV would therefore be 1.8×10^{-4}, which is very close to the required value.

3. PROTOTYPE CONSTRUCTION

A prototype monitor detector using method 4 has been built and tested at the LINAC neutron source at AERE Harwell. Figure 1 shows the basic design of the detector which used a thin aluminised mylar cylinder enclosing the scintillator cube matrix. The matrix was formed by mounting the cubes of scintillator on thin aluminised mylar sheet which was supported across a diameter of the cylinder and together with a reflecting end cap formed the scintillator assembly.

This assembly was end coupled to a forty millimetre diameter photo-multiplier (PM) tube, (EMI 9843). The whole detector assembly together with the PM dynode resistor chain was mounted in a thin aluminium housing to form the complete detector.

The output from the PM was connected to an amplifier/discriminator which provided the signal for the data acquisition electronics.

Results from these preliminary tests demonstrated the principle sufficiently to use the design to monitor the SNS neutron beamlines. To meet this commitment a modification to the design was required in which all hydrogenous material was removed, and other materials reduced to a minimum in order to minimise neutron scattering.

4. PRODUCTION MODEL

Figures 2 and 3 illustrate a design in which all hydrogoneous materials have been replaced by a thin aluminium frame, and glass fibre scintillator support. This support structure is fabricated from 50 micron Al foil and the scintillator cubes glued to 25 micron glass fibres with LOCTITE 358 UV curing adhesive. This assembly is then glued, with Araldite resin, onto the face of the PM tube and surrounded by a 9 micron aluminium foil reflector. The whole structure together with the PM high voltage dynode chain is located in an aluminium tubular housing.

This housing is designed to be placed in a vacuum if required and the length of the neutron beam window is machined to suit different sized detector lengths.

To obtain good immunity from gamma radiation it is essential to obtain a good pulse height resolution; it is then possible to use pulse height discrimination to exclude gamma counts.

Aluminised mylar is a very good optical reflector, but unfortunately cannot be used in this design because of the hydrogen contained in the mylar. Although aluminium foil is inferior, as a reflector, to mylar it must be substituted in the production design, but care must be used in selecting foil with a high quality surface finish.

5. RESULTS FROM PRODUCTION MODEL

Figure 4 shows the neutron pulse height spectrum when the monitor was exposed to a PuBe laboratory source. The important feature is the gap between the noise peak and the neutron peak; this allows operation on a good plateau which provides good stability.

The neutron peak is cut off at the high level end because the amplifier saturated due to large signal pulses.

Figure 5 shows a pulse height spectrum on a log scale, with the detector exposed to ^{60}Co gamma rays, and a few neutron counts to mark the neutron pulse height position. The spectrum shows that there is no overlap of gamma and neutron pulse heights. This situation allows very good discrimination against gamma rays with a measured gamma ray detection efficiency of $< 10^{-8}$.

Subsequent installation of thirteen monitors on SNS beamlines to monitor the first extracted neutrons proved the system successful. For this purpose the detection efficiences were taylored to be ~1% to ensure good count rates at the low beam intensities encountered at the SNS start up.

6. RESULTS FROM SNS BEAMLINES

Figure 6 shows some typical time of flight spectra from two of the neutron beamlines.

Figure 6(a) is from the High Energy Transfer (HET) instrument and shows the response from time zero.

Figure 6(b) and (c) are from the High Resolution Powder Diffractometer (HRPD), which show spectra from the two monitors, one in front of the instrument (b) and one behind (c). The instrument is at the end of a long curved guide which eliminates the high energy neutrons from the beam. This is illustrated by the difference at early times between the HRPD and HET monitors.

The structure on (c) is a result of absorbtion of the neutrons as they pass through various absorbtion foils and scattering samples placed in the path of the beam. By comparison, (b) being before the instrument, exhibits none of these characteristics.

7. CONCLUSIONS

The design of neutron beamline monitor described in this report has been shown to perform to the required specification, giving a smooth response over the thermal and epithermal range of neutron energies.

Efficiences can be varied down to 10^{-4} with the possibility of attaining 10^{-5} using natural lithium in the scintillator instead of Li^{6}. Sensitivity to gamma rays has been measured as less than 10^{-8}.

With the exception of the scintillator, the detector uses standard components and materials, resulting in an inexpensive and easily manufactured monitor.

ACKNOWLEDGEMENTS

The author would like to thank the members of Neutron Division for their discussion and help in testing the monitor detectors and special thanks to Mr H Wroe for his consultation and encouragement.

P L DAVIDSON

8.3.85

Appendix

CONSTRUCTION DETAILS

1. SCINTILLATOR CUBES

Scintillator cubes of 0.25 → 0.3 mm sides can be cut using a thin (0.010 ins) diamond circular saw. The technique is to cement, with resin, a 2 mm piece of scintillator onto a waste piece of glass and cross cut into 0.25 mm squares to a depth of 1.5 mm. The first saw cuts are filled with hard potting resin before the second cross cuts are made. This is illustrated in Figure 7. The matrix formed, is then filled with hard potting resin again and mounted on the sawing machine, as shown in Figure 8, and the saw indexed to cut a .25 mm slice across the matrix.

The resulting slice is soaked in methylene chloride to soften the resin and the cubes of scintillator extracted with tweezers. A low power microscope is an essential aid for this operation.

2. MOUNTING STRUCTURE

Figure 9 shows the scintillator cubes mounted in the holding structure, which, as discussed earlier is constructed from 50 μm aluminium foil. To make the structure strong enough, the foil is rolled round a 1 mm diameter steel rod to form it into a tube. This is then squeezed with tweezers at the corners to allow the tube to bend, and some sections or part sections flattened to allow joints to be made and the glass fibres to be mounted. Figure 9 shows this in detail. Figure 10 shows the assembly mounted on a photomultiplier tube.

The reflecting envelope is formed by wrapping 9 μm aluminium foil round a former to make a tube. The seam is formed by double folding the edges, and the top is prism shaped by careful folding over the top of the former. Figure 11 shows the reflector and the former.

The thickness of the foil is not important from the point of view of obstructing the neutron beam, but the particular foil used had the best reflectivity after mylar, so, is the most important factor in the choice of foil.

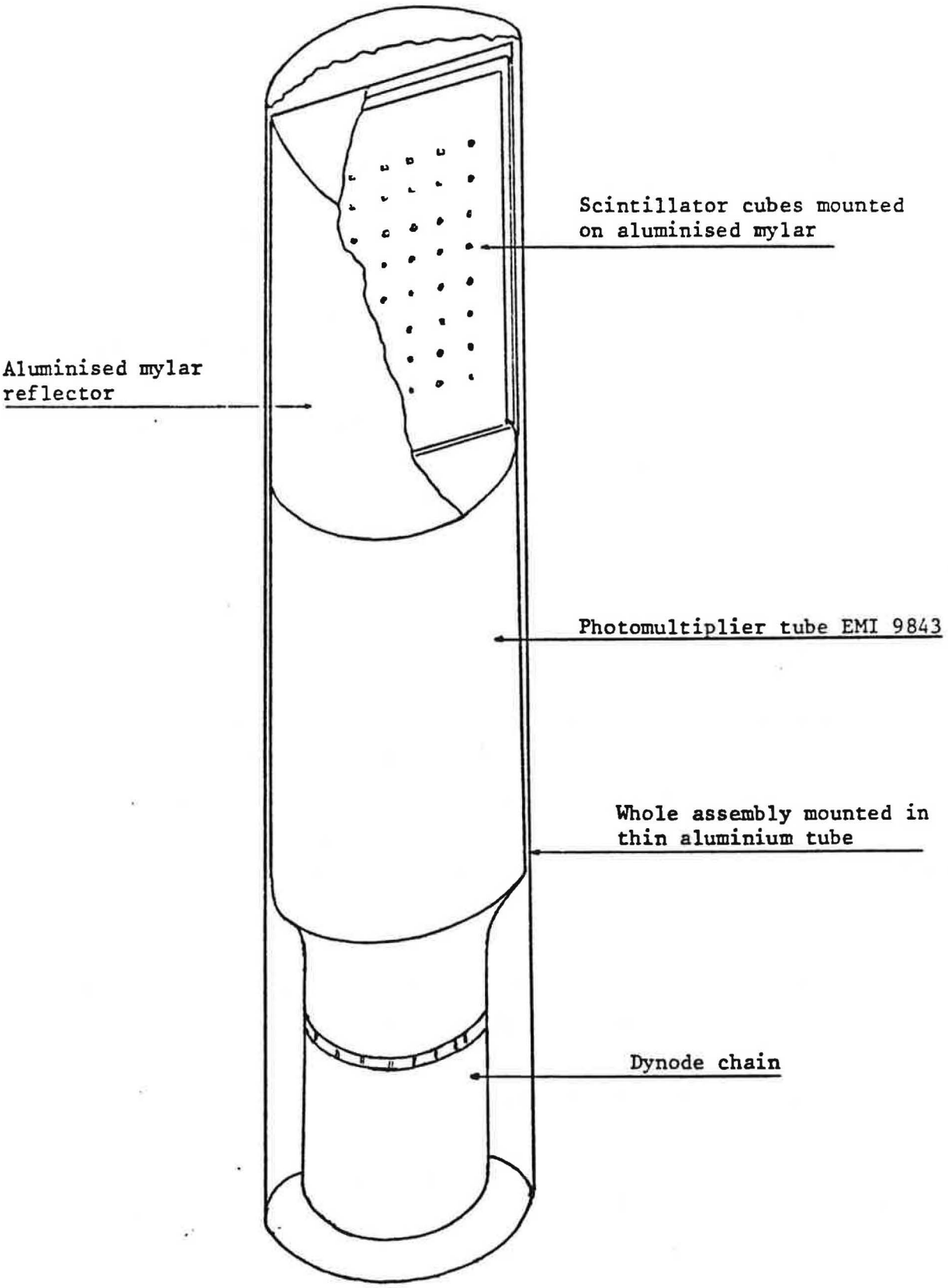

PROTOTYPE DETECTOR

FIGURE 1

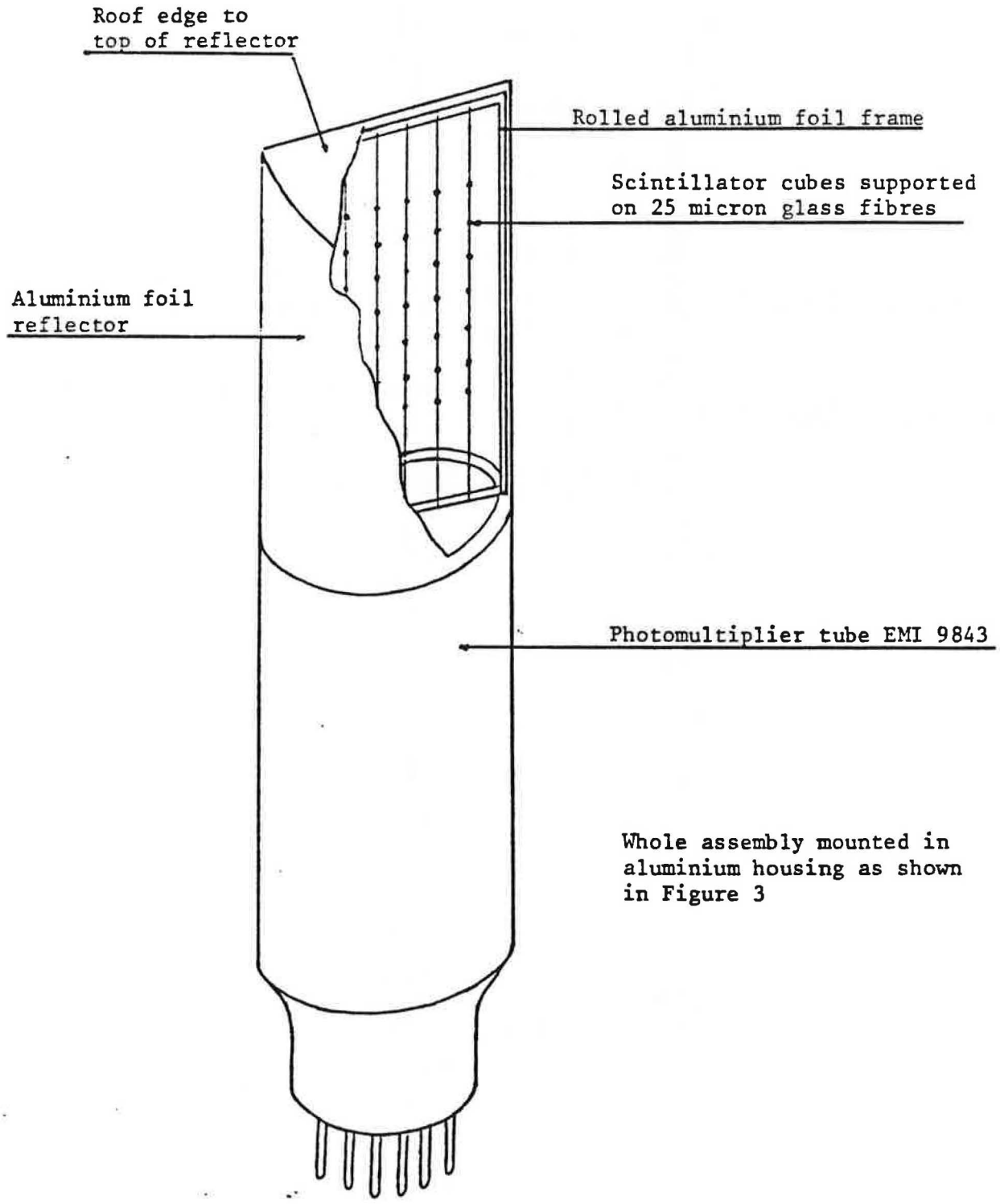

PRODUCTION DETECTOR

FIGURE 2

SCINTILLATION MONITOR DETECTOR

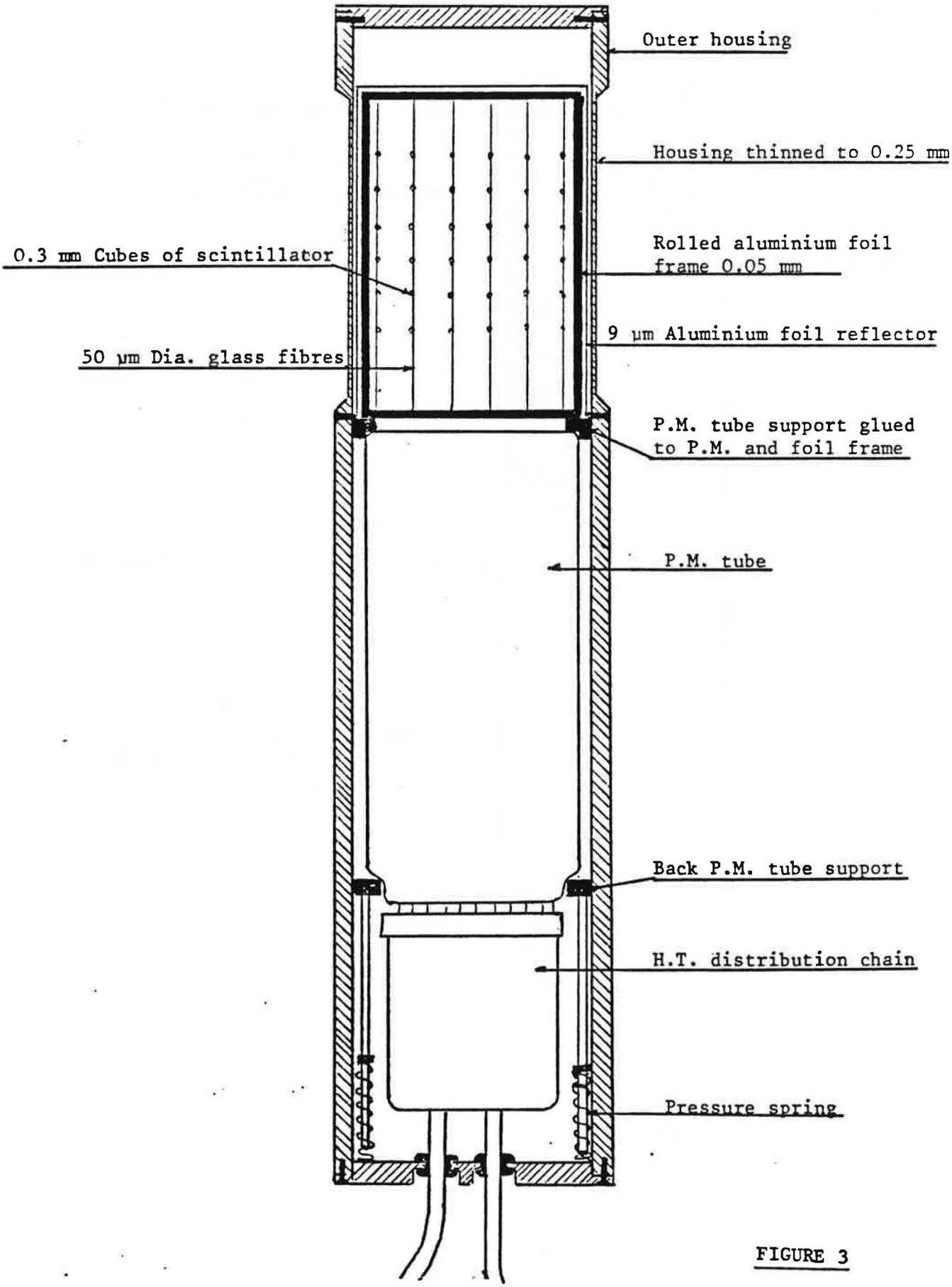

FIGURE 3

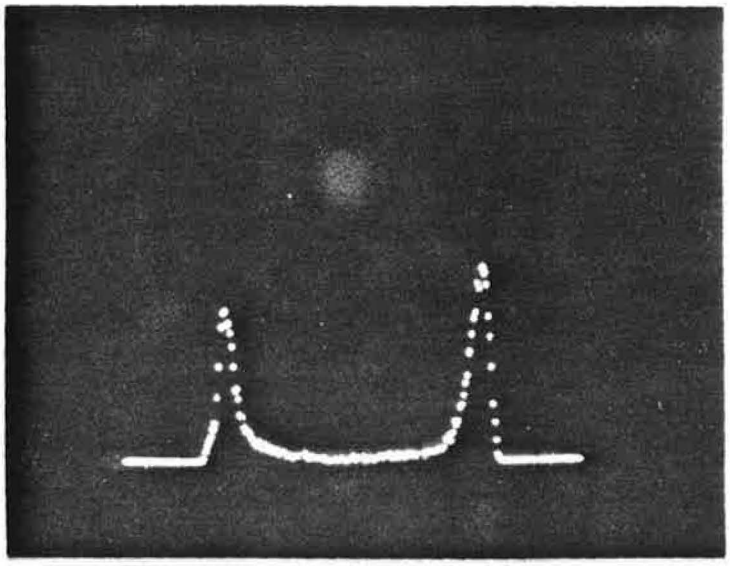

Noise Neutrons

Neutron pulse height spectrum

FIGURE 4

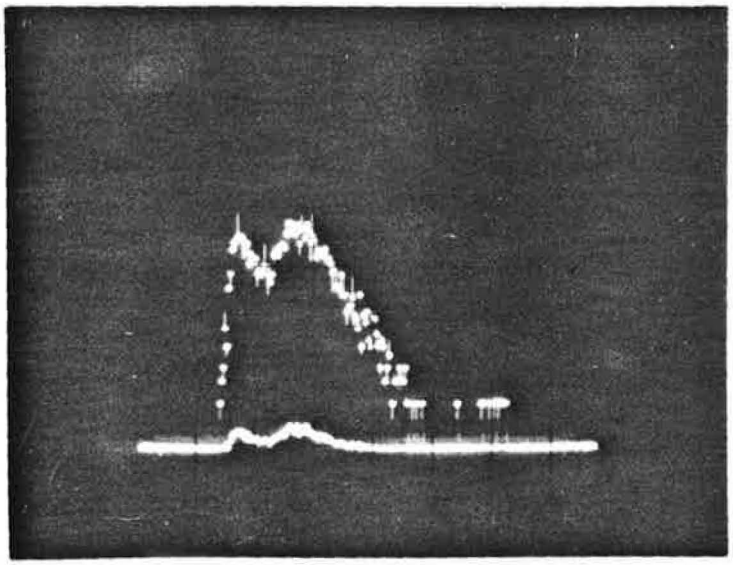

Gamma

Neutrons

Gamma pulse height spectrum plus neutron marker

FIGURE 5

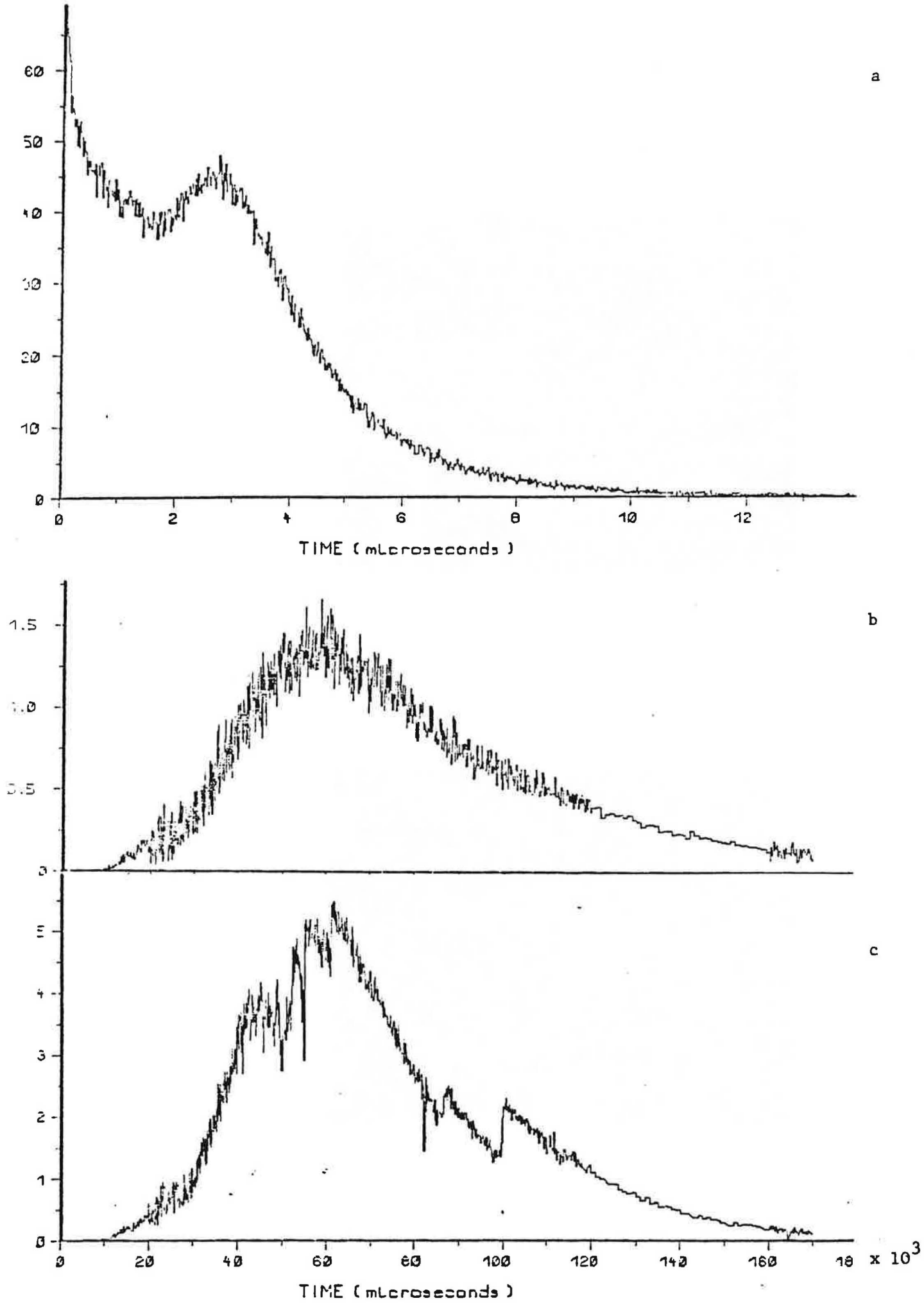

Results from production monitor

FIGURE 6

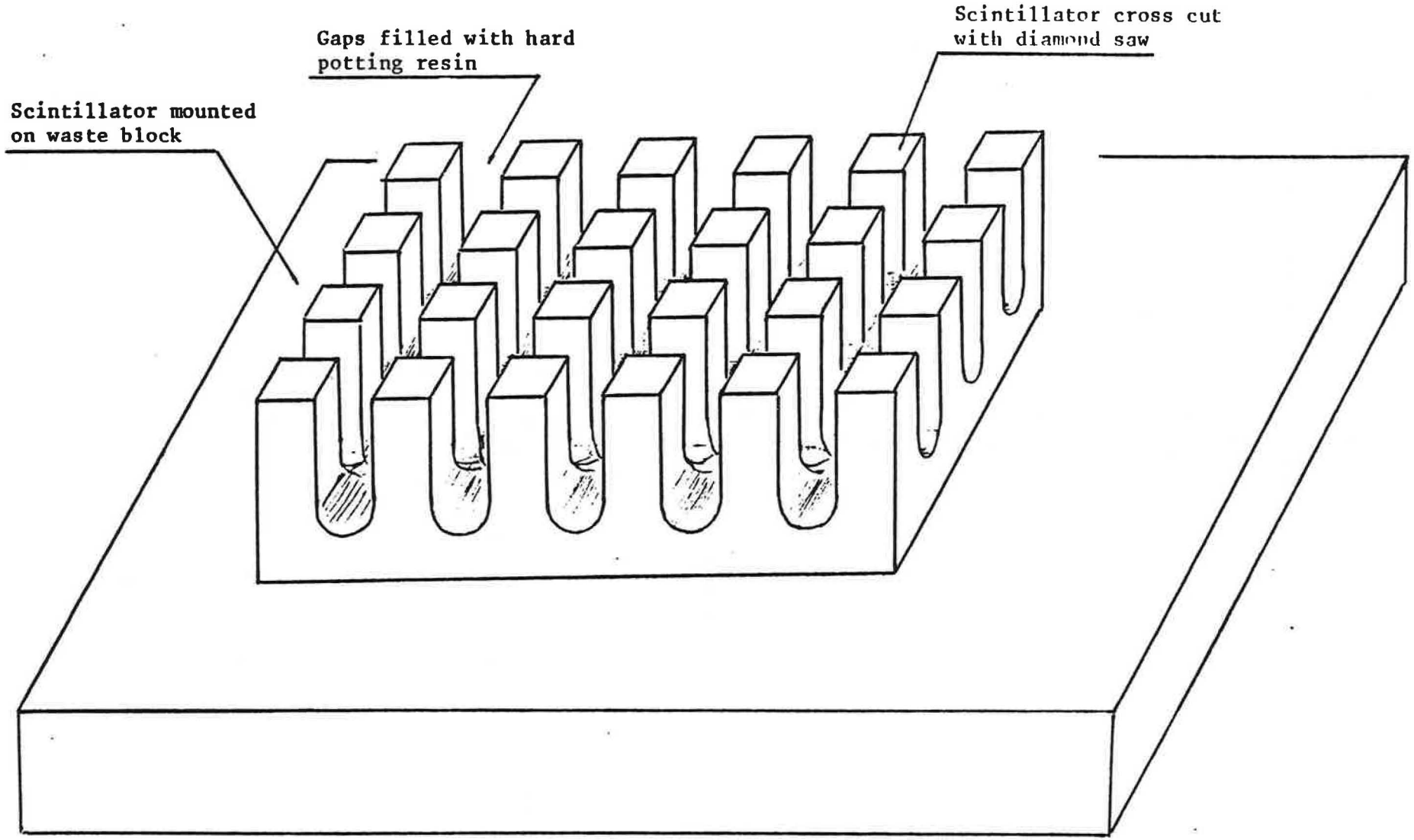

Cube cutting (a)

FIGURE 7

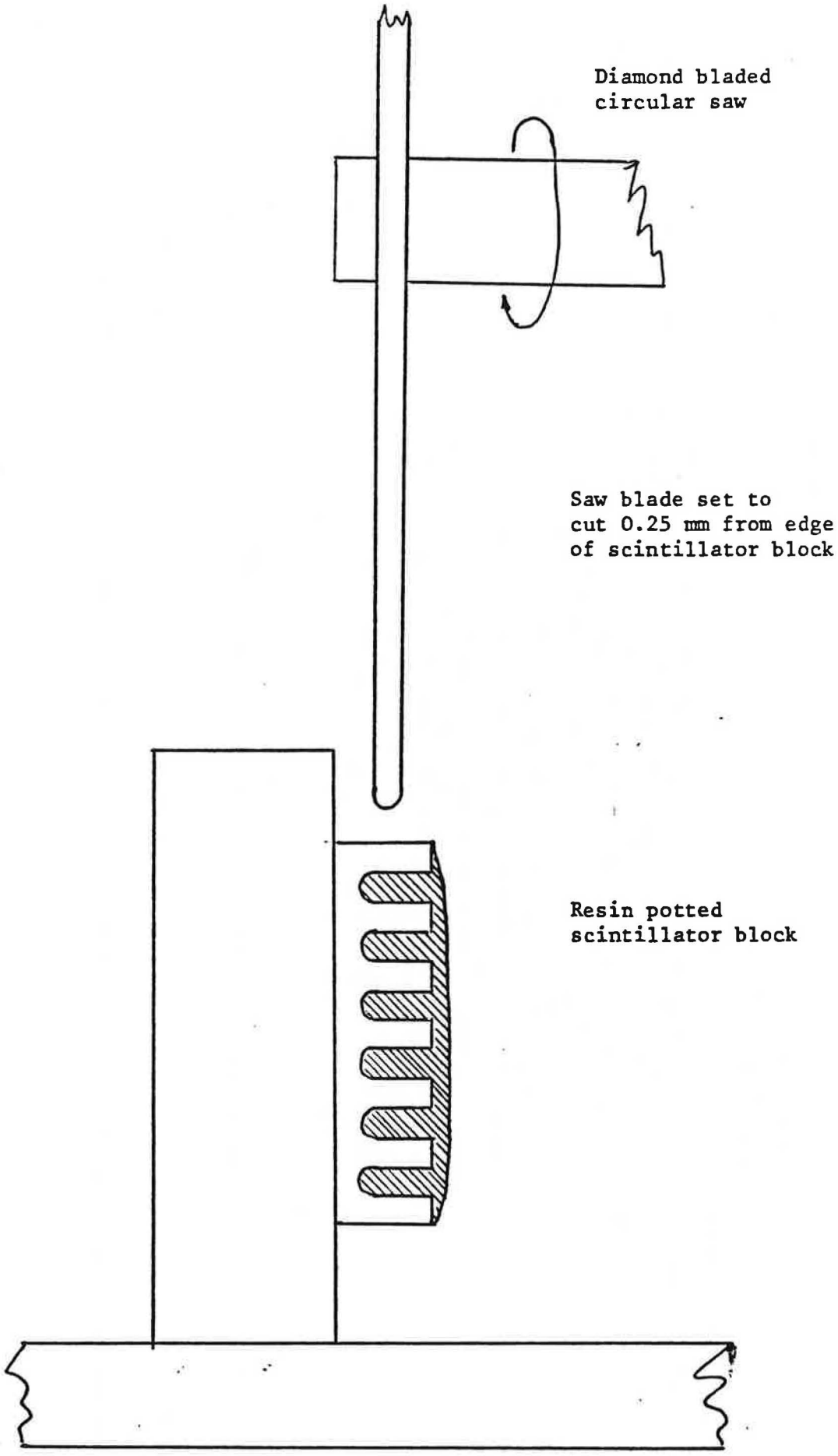

Cube cutting (b)

FIGURE 8

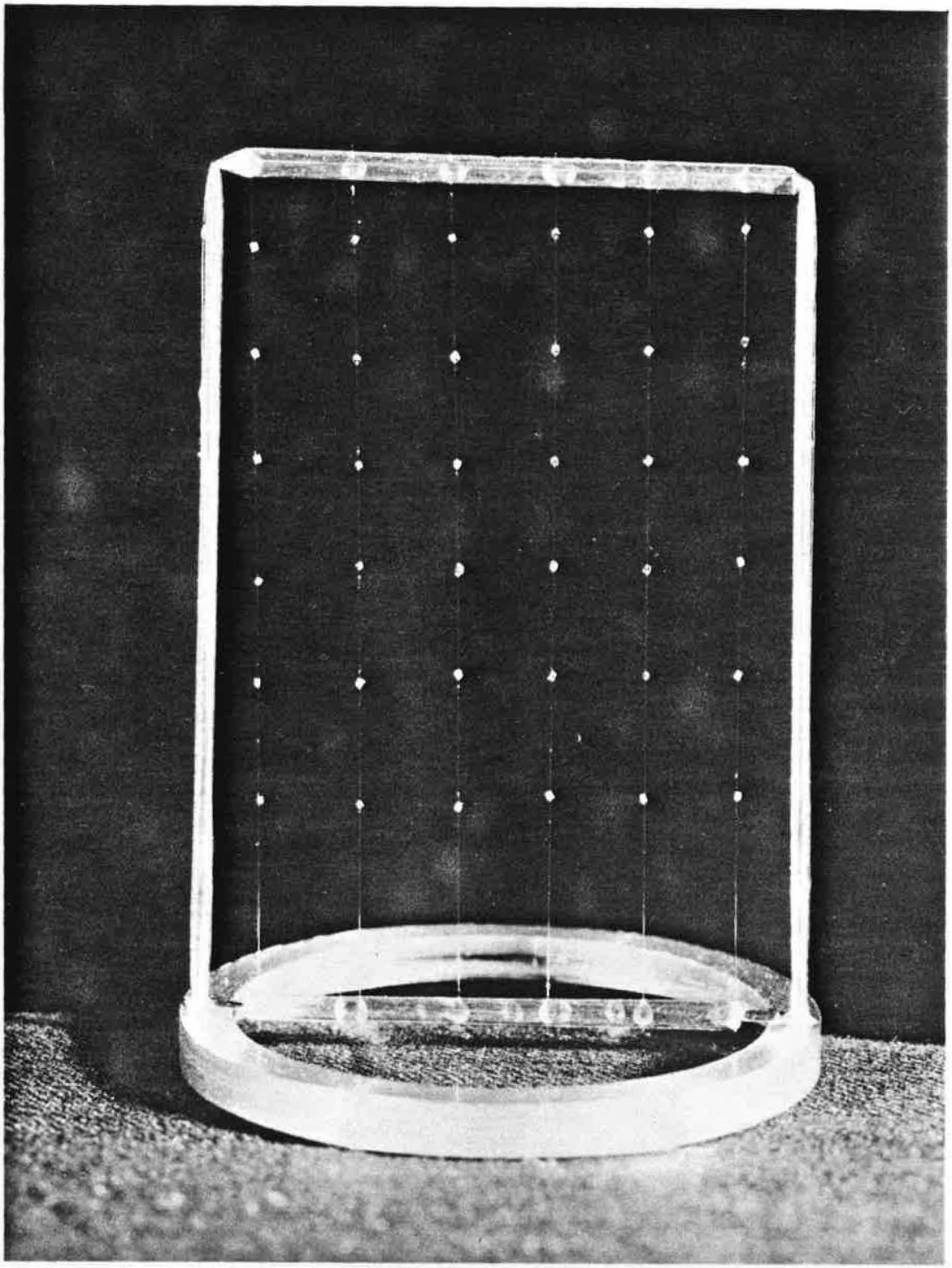

Detailed construction of the scintillator matrix

FIGURE 9

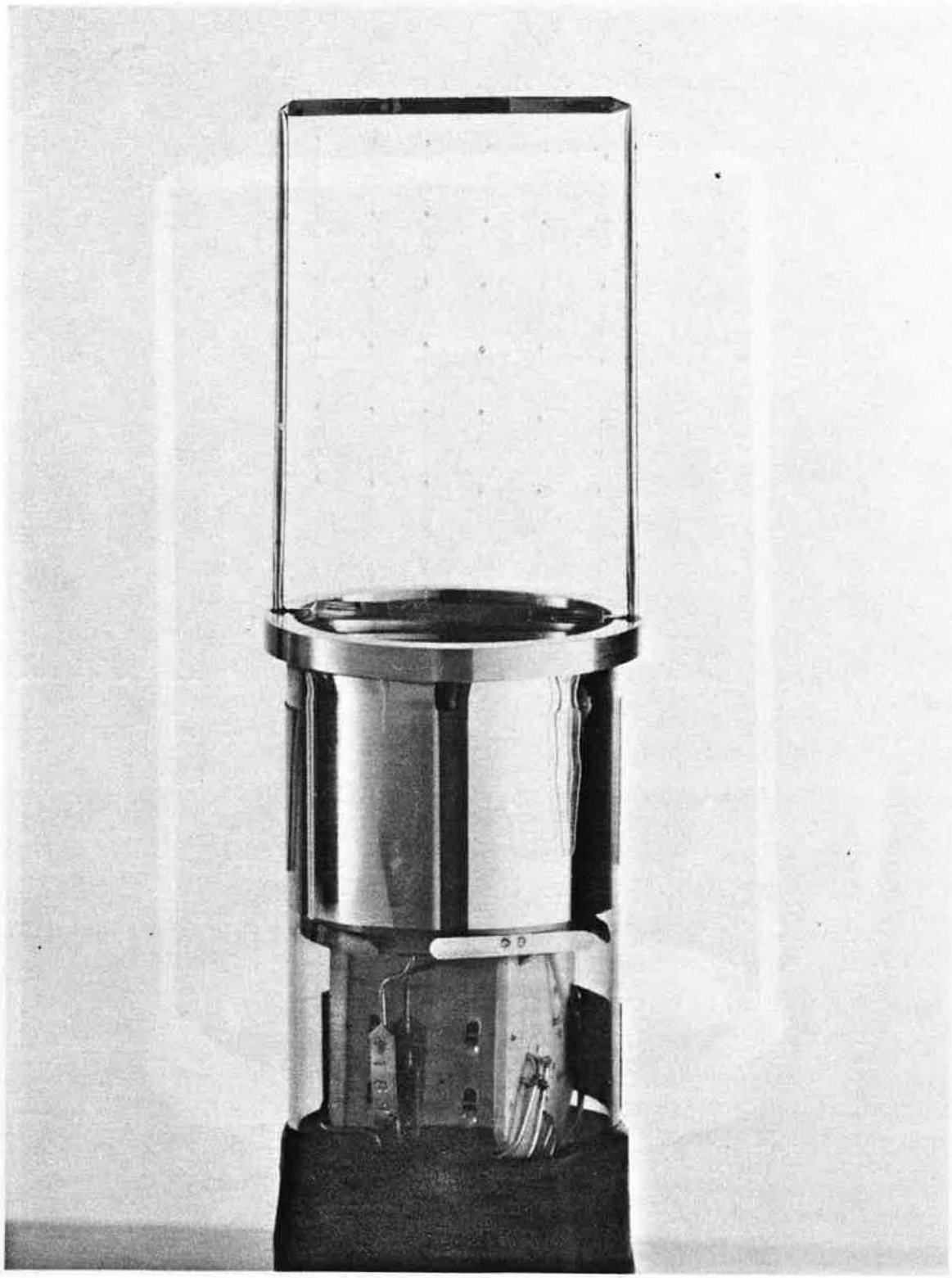

Scintillator assembly mounted on the photomultiplier

FIGURE 10

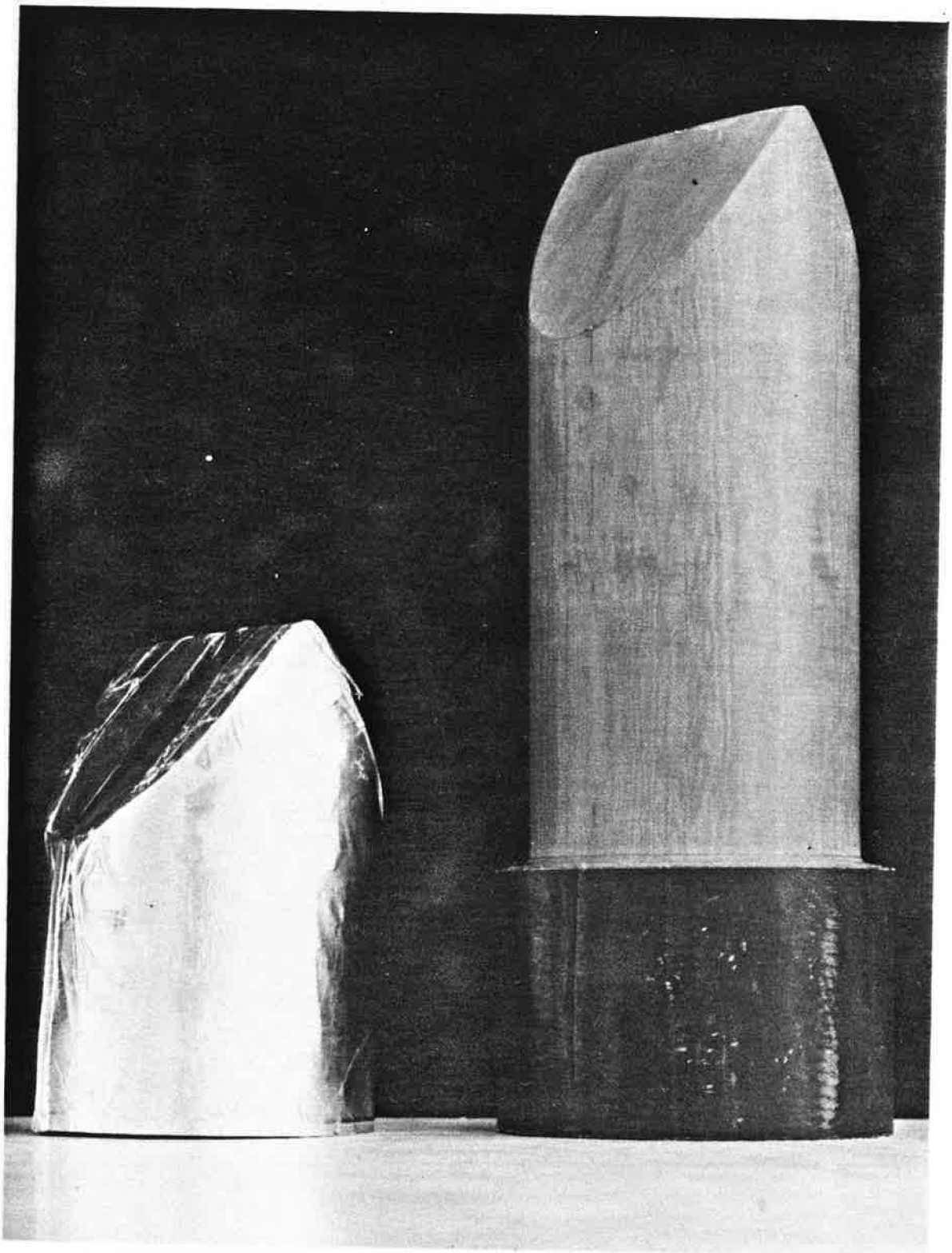

Foil reflector and former on which it is made

FIGURE 11